INSTITUTE OF PHYSICS PUBLISHING NETWORK: COMPUTATION IN NEURAL SYSTEMS

Network: Comput. Neural Syst. **13** (2002) 157–177 PII: S0954-898X(02)33774-6

Burst synchrony patterns in hippocampal pyramidal cell model networks

Victoria Booth[1] **and Amitabha Bose**

Department of Mathematical Sciences, Center for Applied Mathematics and Statistics, New Jersey Institute of Technology, Newark, NJ 07102-1982, USA

E-mail: vbooth@m.njit.edu

Received 17 September 2001
Published 19 March 2002
Online at stacks.iop.org/Network/13/157

Abstract

Types of, mechanisms for and stability of synchrony are discussed in the context of two-compartment CA3 pyramidal cell and interneuron model networks. We show how the strength and timing of inhibitory and excitatory synaptic inputs work together to produce either perfectly synchronized or nearly synchronized oscillations, across different burst or spiking modes of firing. The analysis shows how excitatory inputs tend to desynchronize cells, and how common, slowly decaying inhibition can be used to synchronize them. We also introduce the concept of 'equivalent networks' in which networks with different architectures and synaptic connections display identical firing patterns.

1. Introduction

Although the phrase 'synchronous firing of neurons' is used commonly throughout the literature, its exact meaning is often defined differently depending on the context and on the authors. For example, in describing the sharp wave-associated ripple observed in the CA1 region of the hippocampus, Ylinen *et al* (1995) describe scenarios in which pyramidal cells are synchronized with zero phase lag or in which they are synchronized 'with better than 5 ms precision'. Some authors report on synchronization of spikes (van Vreeswijk *et al* 1994, Ermentrout and Kopell 1998), while others speak about synchronization or near-synchronization of bursts (Traub *et al* 1991, Somers and Kopell 1993, Pinsky and Rinzel 1994, Terman *et al* 1998, Rubin and Terman 2000, Bose *et al* 2000, Booth and Bose 2001a). A mathematical definition of synchronization is that all variables that are used to describe each neuron are identical in all cells for all moments in time. In practice, however, it may be impossible to measure all of these variables and, thus, what is synchronous to one author may not be synchronous to another. For the time being, we shall simply say that two neurons are firing synchronously if their voltage traces are sufficiently close in time.

[1] Author to whom any correspondence should be addressed.

0954-898X/02/020157+21$30.00

An important question is that of what mechanisms are responsible for synchronization of neurons. Many experimental and modelling studies have been performed to determine the effects of different synaptic currents on promoting synchrony. For example, fast excitatory synaptic currents, presumably AMPA mediated, have been shown to synchronize bursting pyramidal cells (Traub *et al* 1991, Pinsky and Rinzel 1994), relaxation oscillators (Somers and Kopell 1993, Bose *et al* 2000) and, if the synapses are very fast, spiking neurons as well (van Vreeswijk *et al* 1994, Hansel *et al* 1995). On the other hand, slowly decaying inhibitory synaptic currents, presumably slow and GABA-B mediated, are also able to maintain synchronous firing in a mutually inhibitory neuronal network (van Vreeswijk *et al* 1994, Gerstner *et al* 1996, Terman *et al* 1998). Given that the CA3 region of the hippocampus, like other hippocampal and cortical regions, is composed of both pyramidal cells with recurrent excitatory collateral connections and inhibitory interneurons that project to both pyramidal cells and other interneurons, it is important to understand the possible synaptic mechanisms that participate in synchronizing firing times.

In this paper, we study how synaptic excitation and inhibition contribute to synchronization of firing in model networks of pyramidal cells and inhibitory interneurons. In the networks, we use the two-compartment model of a CA3 hippocampal pyramidal cell developed by Pinsky and Rinzel (1994). This two-compartment pyramidal cell model together with the rich anatomical structure of the CA3 region provide a setting in which to explore a variety of questions concerning synchronization of pyramidal cells. For example, is synchrony always perfect, or are there other, less precise firing patterns? What are the network properties that lead to perfectly or nearly synchronized firing times? What are the influences of additional synaptic inputs, particularly fast inhibitory inputs, to the pyramidal cells on the synchronous firing pattern?

Recently, we showed that synaptic inhibition arriving during burst firing of a Pinsky–Rinzel pyramidal cell model can modulate the profile of bursts and the frequency of burst firing (Booth and Bose 2001a). Specifically, we showed that when the level of synaptic inhibition is increased, there is a transition in firing pattern from complex bursting, at about 1–2 Hz, to single spiking at about 12 Hz. In larger model networks where the pyramidal cell receives both synaptic excitation and inhibition during a burst, we showed that the transitions in burst firing can be obtained as the net inhibition arriving during a burst varies (Booth and Bose 2001b). An issue that we investigate here is how these effects of local, fast, synaptic inhibition on burst profile and burst frequency modulate synchronous firing of pyramidal cells in pyramidal cell–interneuron model networks.

We consider two primary mechanisms for driving synchronous firing of pyramidal cells: recurrent excitation and common, slowly decaying inhibition. Different model networks are considered in which pyramidal cell firing is synchronized by either of these two mechanisms, or both, and pyramidal cells also receive local, fast inhibitory synaptic inputs. Depending on the network architecture, we find different types of synchronized bursting, such as: (1) 'perfect synchrony' in which burst firing times and burst profiles are exactly the same; (2) 'near synchrony' in which burst firing times are within a short (1–3 ms) time window and burst profiles are similar; and (3) 'burst-envelope synchrony' where burst firing times are within a 1–3 ms time window and burst profiles are different. Analysis of cell firing in the different networks reveals that the type of synaptic input driving synchronization and the relative timing of the local inhibition with respect to the synchronizing synaptic inputs are responsible for the type of synchrony obtained. In the networks considered, the relative timing of the synchronizing inputs and the local inhibition depend on the location of the synaptic inputs, either somatic or dendritic, and on the presence of synaptic delays in the network. We find, in general, that recurrent excitation leads to near-synchronous burst firing or

burst-envelope synchronous firing, while common inhibition can perfectly synchronize firing. Under certain circumstances, we find that recurrent excitation can perfectly synchronize spike firing times. We additionally show that the same relative timing of synaptic inputs, and thus the same synchronous bursting pattern, can be obtained in networks with completely different architectures, where both the number of cells and the synaptic connections are different. This result leads to the concept of 'equivalent networks' where the same dynamics of firing is obtained in different ways by different networks.

The Pinsky–Rinzel pyramidal cell model has been used in a number of hippocampal network studies (Tiesinga *et al* 2001, Menschik *et al* 1999, Wennekers and Sommer 1999, Pinsky and Rinzel 1994, Booth and Bose 2001a). In some of these studies, the influence of particular bursting properties of the model cell on network behaviour has been noted (Tiesinga *et al* 2001, Pinsky and Rinzel 1994). The intent of this study of small networks containing Pinsky–Rinzel model cells is to achieve an understanding of the influence of the intrinsic bursting properties of the cell and the effect of synaptic inputs on those bursting properties on network firing properties. More generally, given the increasing use of multi-compartmental model cells, with active conductances distributed over several compartments, in network studies (for example, Butera *et al* (1999), Traub and Bibbig (2000)), our results may suggest similar influences occurring in networks of different model cells.

2. Model

The model networks that we consider consist of Pinsky–Rinzel pyramidal cells and excitable interneurons. Since the equations and parameter values for the Pinsky–Rinzel model (Pinsky and Rinzel 1994, 1995) and for the interneurons (Booth and Bose 2001a) have been previously described, we refer the reader to the original references and here only briefly describe firing properties of these model cells. Numerical solutions of the model networks were computed using XPP-AUT, a differential equation solver developed by Ermentrout which is freely available on the web (http://www.math.pitt.edu/ bard/xpp/xpp.html1). Files containing our model equations and parameter values in the XPP-AUT format can be found at http://math.njit.edu/~vbooth/.

In our model networks, the Pinsky–Rinzel pyramidal cells are in a very-low-frequency bursting regime (somatic applied current $I_s = 0.75\ \mu\text{A cm}^{-2}$). Briefly, a burst in the two-compartment model is initiated by a fast, sodium spike in the soma compartment that backpropagates to the dendrite and activates a slower, wider calcium-based spike. The dendritic depolarization supports subsequent spikes within the burst. The intrinsic burst has a complex profile with high-frequency, damped spiking in the middle caused by overdriving of the somatic spike generator by dendritic depolarization. The burst ends when the calcium-based spike ends in the dendrite and a calcium-dependent K^+-'afterhyperpolarization' (AHP) current (I_{K-AHP}) contributes to the length of the subsequent interburst interval. Interneurons are modelled as generic, one-compartment excitable cells by the Morris–Lecar equations (Morris and Lecar (1981); see Booth and Bose (2001a) for parameter values).

In the voltage differential equations for the pyramidal cells (either somatic or dendritic voltage) and for the interneurons, post-synaptic currents are modelled by terms of the form $-g_x s_x(V_{post} - V_x)$ where V_{post} is the post-synaptic voltage. The subscript x indicates the specific current with $x = exc$ for recurrent excitatory currents between the pyramidal cells, $x = inh$ for inhibitory currents post-synaptic to the individual pyramidal cells from interneurons local to individual pyramidal cells and $x = inh_c$ for inhibitory currents that are common to both pyramidal cells from a common interneuron. Values for the maximal conductances of recurrent excitation g_{exc} and local inhibition g_{inh} are given in the text and

figure captions for the different networks. The maximal conductance of the common synaptic inhibition is $g_{inh_c} = 1$ mS cm^{-2}. The reversal potentials for excitatory and inhibitory synaptic currents are $V_{exc} = 0$ and $V_{inh} = -80$ mV, respectively. The gating variables for the synaptic currents are governed by equations of the form

$$s_x' = \alpha_x H_\infty(V_{pre} - V_\theta)[1 - s_x] - \beta_x H_\infty(V_\theta - V_{pre})s_x,$$

where V_{pre} is pre-synaptic voltage. The Heaviside function, H_∞, is used to enforce the synaptic threshold at $V_\theta = -10$ mV. In other models of synaptic current, the decay term does not include a Heaviside function. We include it for mathematical convenience and its presence does not change our results. The constants α_x and β_x are the rise and decay rates of the synaptic currents. Recurrent excitation between the pyramidal cells mimics AMPA-mediated excitatory currents with fast activation and decay ($\alpha_{exc} = 2$ and $\beta_{exc} = 1$ m s^{-1}). The inhibitory currents from interneurons local to the pyramidal cells are similar to fast GABA-A-mediated currents ($\alpha_{inh} = 2$ and $\beta_{inh} = 0.1$ m s^{-1}) while the common inhibitory current is more like a slowly decaying GABA-B-mediated current ($\alpha_{inh_c} = 2$ m s^{-1} and β_{inh_c} ranges from 0.05 to 0.0001 m s^{-1} with specific values given in the text). The excitatory synaptic currents from the pyramidal cells to the local and common interneurons are identical to the fast, recurrent excitatory currents between the pyramidal cells except that the maximal conductances are set higher, to 5 mS cm^{-2}, to ensure interneuron firing. Synaptic delays, when present in a network, are incorporated as a fixed-length time delay in the synaptic gating variable s_x in the post-synaptic current term (an automatic feature of XPP-AUT).

All the networks that we consider contain a subcircuit consisting of a Pinsky–Rinzel pyramidal cell with reciprocal synaptic connections to an excitable interneuron, where the synaptic currents are modelled as described above. When the pyramidal cell is in the very-low-frequency bursting regime, the interneuron provides fast, inhibitory input during the burst which, as we have shown previously, modifies the burst profile and burst frequency (Booth and Bose 2001a). Specifically, when the strength of the inhibitory current (g_{inh} in the networks) is weak, the pyramidal cells fire complex bursts at slightly higher frequencies than the intrinsic burst frequency. As g_{inh} increases, there is a smooth transition in burst profiles from complex bursting to bursts with four spikes, then to bursts with three spikes, then to spike doublets and finally to single spikes for large values of g_{inh}. With the change to each burst mode, interburst intervals get shorter, leading to increasing burst frequency. The changes in burst profile and frequency are caused by suppression of the dendritic calcium spike underlying the burst. Attenuated dendritic depolarization cannot support as many somatic spikes in the burst and also results in less activation of I_{K-AHP}. Thus, as the strength of inhibitory input arriving during the burst increases, the number of spikes per burst decreases and the subsequent interburst interval gets shorter.

3. Results

3.1. Recurrent excitation cannot maintain perfect synchrony of burst firing

Pinsky and Rinzel (1994), for large networks consisting of their two-compartment model pyramidal cells randomly connected with fast, excitatory synapses, and Traub *et al* (1991), for similar networks consisting of their 19-compartment pyramidal cell model, found that excitatory synaptic connections among the cells lead to firing times that are not exactly synchronized. Similarly, we find in small networks consisting of Pinsky–Rinzel pyramidal cells and excitable interneurons where fast, recurrent synaptic excitation among pyramidal cells is the primary synchronizing mechanism that perfectly synchronous bursting is not stable. Instead, such networks display near-synchronous bursting or burst-envelope synchronous firing. Excitation can, however, under certain circumstances, perfectly synchronize spikes.

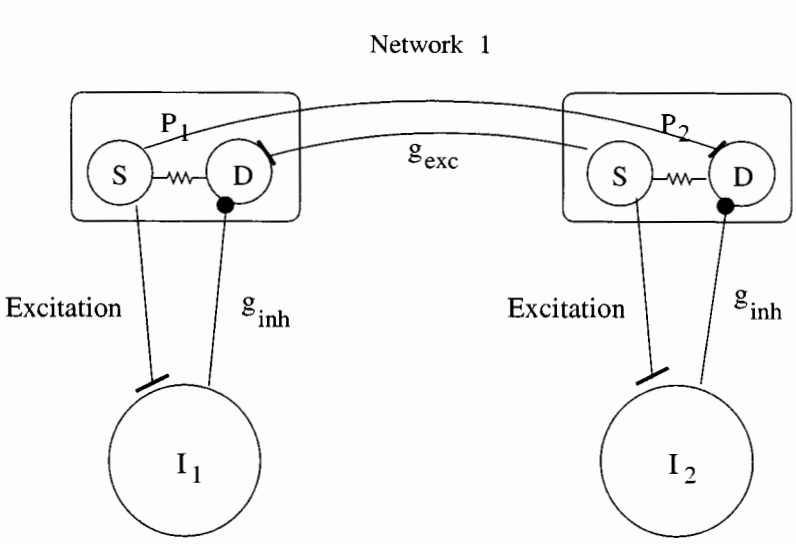

Figure 1. (*a*) A schematic diagram of model network 1. (*b*)–(*f*) Pyramidal cell somatic voltage traces of near-synchronous bursting modes as maximal conductances of recurrent excitatory synaptic currents, g_{exc} in mS cm^{-2}, are varied. Maximal conductance of local inhibitory synaptic current g_{inh} = 0.7 mS cm^{-2} (solid traces: leader cell; dotted traces: follower cell; dashed lines illustrate separation in firing times). (*g*), (*h*) Pyramidal cell somatic voltage traces (first panel), dendritic voltage traces (middle panel) and post-synaptic currents (third panel) for the leader cell (solid traces) and follower cell (dotted traces) for g_{exc} = 3.5 when g_{inh} = 0 (*g*) and g_{inh} = 0.7 mS cm^{-2} (*h*). Arrows in middle panels indicate times of peak excitatory (upward-pointing arrows) and inhibitory (downward-pointing arrows) post-synaptic currents in the leader cell (solid arrows) and the follower cell (dotted arrows).

3.1.1. Near-synchronous bursting. When two Pinsky–Rinzel pyramidal cells are connected via fast excitatory synapses to the dendritic compartments of the pyramidal cells, near-synchronous bursting is obtained. Both cells fire complex bursts with one cell leading burst firing approximately 2 ms ahead of the follower cell. This near-synchronous bursting can be maintained when the burst profile and burst frequency are modulated by fast inhibition arriving during the burst. An example network where this is achieved consists of two pyramidal cell–interneuron subcircuits coupled by fast, recurrent excitation targeting the dendrite compartments of the pyramidal cells (network 1, figure 1(*a*)). As the strength of the excitatory synapse between the pyramidal cells is weakened, so that net inhibition to the pyramidal cells increases, near-synchrony is maintained as the burst profile changes and the interburst interval shortens (figures 1(*b*)–(*f*)). The time separation between firing of the pyramidal cells remains approximately 2 ms with a slight increase to about 3 ms when excitation is very weak and the pyramidal cells fire single spikes. The transitions in burst profile in the two cells are the same except when g_{exc} = 2.6 in which case the leader cell fires a burst with four spikes and the follower cell fires a complex-like burst with three spikes (figure 1(*c*)).

While synaptic excitation keeps firing times of the pyramidal cells close, it is not a fully synchronizing agent for these cells. In a separate paper (Bose and Booth 2002), we prove that perfectly synchronous bursting is unstable in network 1 in the presence and absence of local inhibition. Here, we can gain a qualitative understanding of the slight desynchronizing effect of excitation that keeps firing times separated by considering the dendritic voltages during burst firing (figure 1(*g*)). When local inhibition is absent in the network, the burst profiles are

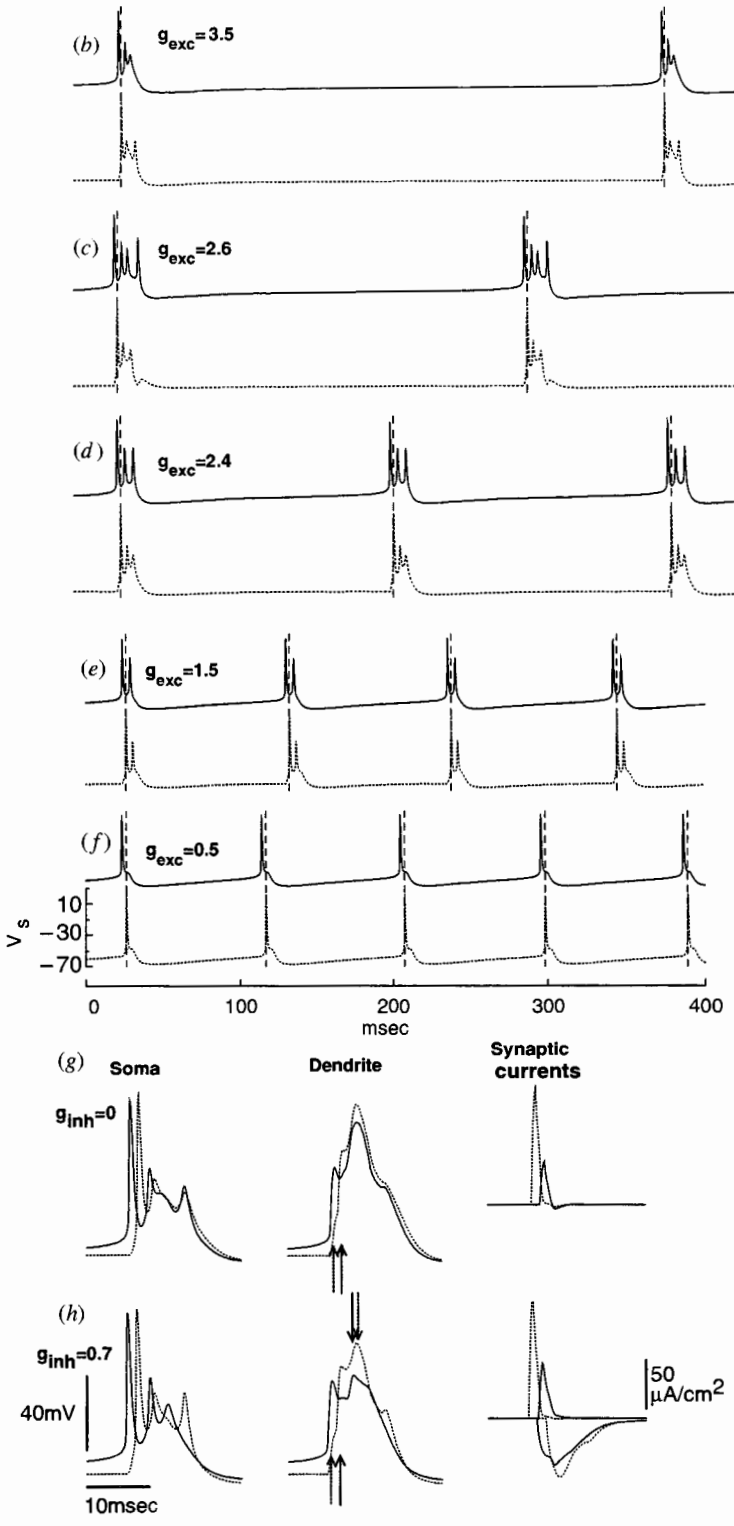

Figure 1. (Continued.)

very similar, but there is a 5–10 mV difference in peak dendritic voltage during the burst with the higher dendritic voltage in the follower cell (figure 1(*g*), middle panel). This difference in dendritic voltage is due to the different mechanisms stimulating the calcium-based spike in the dendrite of the leader and the follower cell.

In the leader cell (figure 1(*g*), solid traces), the burst is initiated by a somatic sodium spike that backpropagates to elicit the dendritic spike and also triggers the synaptic current to the follower pyramidal cell. In the follower cell (dotted traces), on the other hand, the dendritic calcium spike is initiated by synaptic excitation from the leader cell (middle panel, dotted upward-pointing arrow). When the synaptic strength is large, this more direct stimulation of the dendrite causes a faster activation and a larger peak of the calcium spike than if the spike were stimulated by backpropagating somatic depolarization. As a result, peak intracellular calcium and peak K^+-AHP current amplitude are larger in the bursts of the follower cell than in the leader cell. A consequence of more K^+-AHP current activated during the burst of the follower cell is that its subsequent interburst interval is longer than for the leader cell (Booth and Bose 2001a). Thus, the next burst is again initiated by the leader cell and the follower cell remains the follower.

When local inhibition is present in the network, similarly, perfectly synchronous bursting is unstable because of differences in peak dendritic voltage in the leader and follower cells (figure 1(*h*), middle panel). Again, this difference is caused by the difference in stimulation of the dendritic calcium spike. In this case, the somatic versus dendritic stimulation of the spike also causes a difference in the relative timing of the recurrent excitation and local inhibition in the leader and follower cells (figure 1(*h*), third panel). The difference in relative timing of synaptic inputs contributes to the differences in dendritic depolarization. For example in network 1, the initial sodium spike of the leader cell triggers the synaptic currents to the leader interneuron and to the follower pyramidal cell. In response to the synaptic excitation, the leader interneuron inhibits the dendrite of the leader cell (figure 1(*h*), middle panel, solid downward-pointing arrow), and the follower pyramidal cell excites the dendrite of the leader (solid upward-pointing arrow). As there are no synaptic delays in the network and both synapses are fast activating, this excitation and inhibition arrive at approximately the same time (third panel, solid traces). Since the activation of the dendritic calcium current is slow, the excitation and inhibition arrive before the calcium conductance has been fully activated and can modulate its peak amplitude (compare to figure 1(*g*), middle panel, solid trace).

In the follower cell, on the other hand, the synaptic excitation from the leader cell arrives first, initiating the burst (figure 1(*h*), middle panel, dotted upward-pointing arrow). When recurrent excitation is strong, the dendrite is sufficiently depolarized that the local inhibition does not have a significant effect on the burst (dotted downward-pointing arrow). So, although the follower receives greater net inhibition during the burst than the leader cell, the inhibition arrives when the dendrite is sufficiently depolarized that it does not modulate peak voltage effectively. When the strength of recurrent excitation is decreased, with the result that net inhibition to the pyramidal cells increases, the peak dendritic voltages in both the leader and follower cells are attenuated, leading to modulation of the burst profiles. In the leader cell, the attenuation is a result of an increase in net inhibitory input arriving during the burst caused by the combination of weaker recurrent excitation and a fixed level of local inhibition. In the follower cell, weaker recurrent excitation does not depolarize the dendrite as much, so suppression by local inhibition does modulate the burst profile.

In this network, the bursting frequency in each burst mode is determined by the leader pyramidal cell–interneuron subcircuit. As a result, the frequencies for each burst mode are very similar to the frequencies displayed by an isolated pyramidal cell–interneuron subcircuit, as shown in table 1.

Table 1. Frequencies of stable burst firing in each burst mode. Burst modes are changed by varying the strength of the local inhibition, g_{inh}, in the P–I subcircuit, and by varying the strength of the recurrent excitation, g_{exc}, in networks 1 and 2. Values of g_{inh} in the P–I subcircuit and g_{exc} in networks 1 and 2, respectively, for the different burst modes are: complex bursts: (0–0.21, 3.5–3.0, 3.5–2.3); four-spike bursts: (0.28–0.3, 2.7–2.6, 2.1–1.6); three-spike bursts: (0.32–0.34, 2.5–2.4, 1.4–1.2); spike doublets: (0.37–0.5, 1.5–1.2, 1.0–0.6); and single spikes: (0.54–0.7, 0.7–0, 0.4–0) in mS cm^{-2}.

	Bursting frequency (Hz)		
Burst mode	P–I subcircuit	Network 1	Network 2
Complex bursts	2.0–3.0	3.3–3.4	5.6–5.8
Four-spike bursts	3.3–4.1	3.7–4.3	5.9–6.9
Three-spike bursts	5.9–6.7	5.6–6.5	7.9–9.0
Spike doublets	8.1–9.9	9.4–10.0	9.6–10.5
Single spikes	10.9–11.1	10.9–11.1	10.9–11.1

3.1.2. Burst-envelope synchrony. In network 1 considered above, we argued that a factor contributing to the instability of perfectly synchronized bursting was the difference between the mechanisms that stimulate the dendritic calcium spike in the two pyramidal cells. When recurrent excitation targets the soma compartments of two mutually coupled pyramidal cells, the dendritic spikes in both cells are stimulated by backpropagation of a somatic spike. However, perfectly synchronous bursting is not stable in this network either (figure 2(*g*)). Instead, the cells display a near-synchronous bursting pattern where each cell fires a complex burst and they alternate initiating firing each cycle. The somatic burst profiles are not identical in the cells, with the leader cell firing a complex burst similar to the burst of an isolated cell and the follower cell firing a much wider burst consisting of more spikes.

The cause of this difference in burst profile can be understood by again considering dendritic voltages (figure 2(*g*), middle panel). In the leader cell (solid trace), the dendritic calcium spike is fully activated as expected, since the recurrent excitation arriving after the initial spike (third panel and first panel, solid upward-pointing arrow) only enhances somatic and dendritic depolarization. The follower cell should be expected to fire a burst very similar to an isolated burst since the recurrent excitation to the soma (first panel, dotted upward-pointing arrow) stimulates the initial spike that then backpropagates to the dendrite. Instead, after the initial spike, the somatic voltage in the follower cell (first panel, dotted trace) shows a slight suppression which hinders the backpropagating depolarization and, hence, the activation of the dendritic calcium spike (middle panel, dotted trace). This slight suppression is caused by the reversal of the excitatory synaptic current at the peak of the initial spike (third panel, dotted trace). As in previous models of AMPA-mediated synaptic currents, the reversal potential is set to 0 mV (Pinsky and Rinzel 1994, Tiesinga *et al* 2001) and the initial somatic spike peaks at about 12 mV. Since the dendritic calcium spike does not fully activate immediately, the moderately depolarized dendrite can support additional somatic spikes and only when the dendrite depolarizes further do the dendritic potassium currents activate to bring voltage down. A consequence of the smaller dendritic peak voltage is less build-up of intracellular calcium and, hence, less activation of I_{K-AHP}. Thus, the follower cell's subsequent interburst interval is shorter than that for the leader cell and the follower initiates the next burst. When the excitatory reversal potential is set higher, say at 20 mV, then the pyramidal cells fire more synchronously and their burst profiles are very similar. Note that the excitatory synaptic current in the leader cell does not show any reversal since it arrives after the initial spike (figure 2(*g*), first panel, solid upward-pointing arrow) when voltage is well below 0 mV.

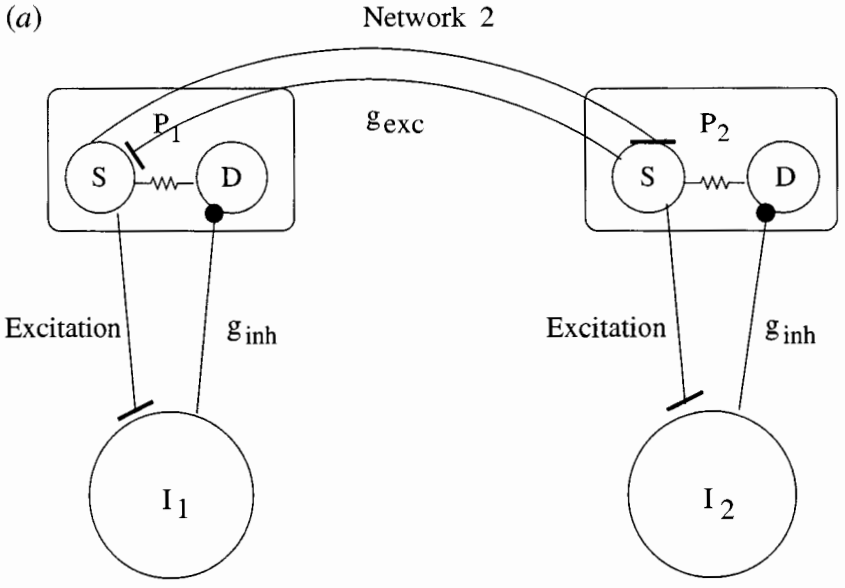

Figure 2. (*a*) A schematic diagram of model network 2. (*b*)–(*f*) Pyramidal cell somatic voltage traces of burst-envelope synchronous firing in different bursting modes as maximal conductances of recurrent excitatory synaptic currents, g_{exc} in mS cm^{-2}, are varied (g_{inh} = 0.7 mS cm^{-2}). (*g*), (*h*) Pyramidal cell somatic voltage traces (first panel), dendritic voltage traces (middle panel) and post-synaptic currents (third panel) for the leader cell (solid traces) and follower cell (dotted traces) for g_{exc} = 3.5 when g_{inh} = 0 (*g*) and g_{inh} = 0.7 mS cm^{-2} (*h*). (*g*) Third panel: note that the excitatory post-synaptic current in the follower cell (dotted trace) briefly reverses following initial activation (indicated by ∗). (*h*) Third panel: post-synaptic current traces for leader cell (upper, solid traces) and follower cell (lower, dotted traces) are offset for clarity. Upward-pointing (downward-pointing) arrows in the first (middle) panels indicate the time of peak excitatory (inhibitory) post-synaptic currents in the somatic (dendritic) compartment of the leader cell (solid arrows) and the follower cell (dotted arrows).

In a network where each pyramidal cell also receives synaptic inhibition from reciprocally connected local interneurons (network 2, figure 2(*a*)), burst-envelope synchronous firing is displayed (figures 2(*b*)–(*f*)). Now, the result of the local inhibition is a different modulation of the burst profile and the subsequent interburst interval in the two pyramidal cells. Specifically, with strong recurrent excitation (figure 2(*b*)), the cells alternate initiating firing and they show an alternation in burst profiles. The leading cell fires a complex burst and the follower fires a single spike. On the next burst cycle, the follower cell becomes the leader and fires a complex burst, and the previous leader cell fires a single spike shortly after the bursting cell. As the strength of recurrent excitation, g_{exc}, is continuously decreased (figures 2(*c*)–(*f*)), the leading cell's burst profile changes while the follower cell consistently fires single spikes. If the recurrent excitation is very strong compared to the strength of the local inhibition, both cells fire complex bursts on each cycle and they alternate initiating firing, just as when local inhibition is absent.

To understand the desynchronizing effect of excitation in this network, again we look to the dendritic voltages during the burst (figure 2(*h*)). In this case, peak dendritic voltages are similar in the two cells but the dendritic calcium spike is suppressed in the follower cell (middle panel, dotted trace) due to differences in the timing of the recurrent excitation and inhibition in that cell. As in the previous network, the burst in the leader cell is initiated by a

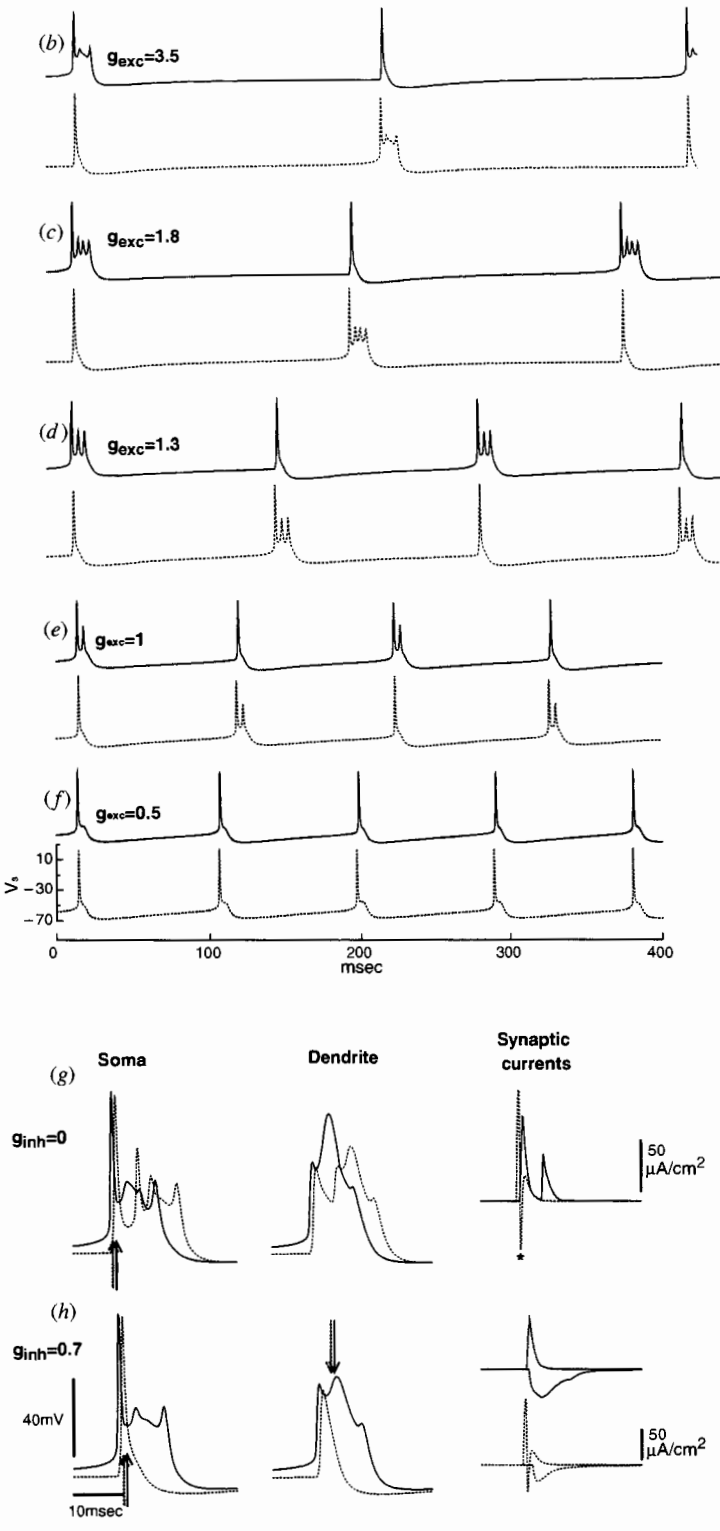

Figure 2. (Continued.)

somatic spike that backpropagates to excite the dendritic calcium spike. The leading sodium spike also triggers synaptic currents to the leader interneuron and to the soma compartment of the follower pyramidal cell. Before the dendritic calcium current is fully activated in the leader cell (middle panel, solid trace), the inhibitory synaptic input arrives (solid downward-pointing arrow) and is able to modulate it. At approximately the same time, the recurrent excitation arrives at the soma compartment (third panel, solid upper traces; first panel, solid upward-pointing arrow). While the maximal conductance of the inhibitory synaptic current g_{inh} is set to a value that when acting alone would suppress the dendritic calcium spike, in the leader cell the backpropagation of the somatic depolarization caused by the recurrent excitation combines with the inhibition to allow partial expression of the dendritic calcium spike. In the follower cell, while there is residual recurrent excitation in the soma compartment (third panel, dotted lower traces) at the time when the inhibitory input from the follower interneuron arrives (middle panel, dotted downward-pointing arrow), the net inhibition is sufficiently strong to suppress its dendritic calcium spike. Thus, the follower cell only fires a single spike. Since the interburst interval following a single spike is shorter than that following a burst, the subsequent burst in the follower cell occurs before the next firing of the leader cell.

When recurrent excitation is weak (for example, $g_{exc} = 0.5$ mS cm^{-2}, figure 2(*f*)), with the result that both cells fire single spikes, firing becomes perfectly synchronized. In this case, both cells receive maximal inhibition during the burst; thus their burst profiles are the same. The recurrent excitation, though weak, can pull firing times together. We note, however, that in this case synaptic mechanisms alone are not responsible for perfectly synchronizing firing times. Obtaining perfect synchrony also depends on intrinsic firing properties of the pyramidal cell, namely dendritic depolarization. To see this, consider network 2 with $g_{inh} = 0$ mS cm^{-2}. If we set the somatic applied current $I_s = 2.5$ μA cm^{-2}, then each pyramidal cell, when isolated, fires high-frequency single spikes, and the dendrite compartment is depolarized, but does not actually spike. In this case, for various values of g_{exc}, the cells do not perfectly synchronize (simulations not shown). If we increase the maximal conductance of the electrotonic coupling between compartments in each cell to $g_c = 11.0$ mS cm^{-2}, then for a range of g_{exc}-values, the cells fire perfectly synchronized spikes. Here, the dendrites fire spikes which are also perfectly synchronized. Alternatively, when recurrent excitation targets the dendrite compartment, the cells fire near-synchronous spikes. Thus, perfect synchrony of spikes depends crucially on the location of the synapse, and also whether or not the dendrite fires a spike. In Bose and Booth (2002), we show why a dendritic spike is necessary for perfect synchronization. In short, a dendritic spike activates the K^+-AHP current whose dynamics is critical to spike time compression.

The population frequencies in this burst-envelope synchronous firing pattern are higher than the frequencies obtained for corresponding burst modes in the near-synchronous bursting pattern (table 1). This difference stems from the fact that each interburst interval is determined by a spiking cell, rather than by a bursting cell.

3.2. Common, delayed, slow inhibition can perfectly synchronize bursting

Similarly to modelling studies with simple one-compartment neuron models (van Vreeswijk *et al* 1994, Gerstner *et al* 1996, Terman *et al* 1998, Rubin and Terman 2000), our study finds that delayed, slowly decaying inhibition that arrives simultaneously at both pyramidal cells can perfectly synchronize their bursting. Additionally, in a network composed of two pyramidal cell–interneuron subcircuits with a common interneuron reciprocally coupled to the pyramidal cells, the common inhibition can maintain perfect synchrony across all firing

modes (network 3, figure 3(*a*)). Since the pyramidal cells are not connected by recurrent excitatory collaterals in this network, the burst mode is varied by directly changing the level of local synaptic inhibition within the pyramidal cell–interneuron subcircuits, g_{inh}. Here, the pyramidal cells receive two sources of synaptic inhibition: local and common. While both the local and common interneurons fire in response to a pyramidal cell burst, since the common inhibition has a delay in its synapse back to the pyramidal cells, these two sources do not act on the pyramidal cell at the same time. Specifically, the local inhibition is fast activating with no synaptic delays, so it arrives at the pyramidal cells during the bursts. It also decays quickly and dissipates near the end of the burst. The effect of this local inhibition is to modulate the burst firing pattern. The common inhibition that acts on both pyramidal cells has a synaptic delay of 20 ms, so the inhibition arrives after the burst (see figure 3(*b*)), well after the local inhibition has decayed. With a slow decay rate of the common inhibition, for example $\beta_{inh_c} = 0.005$ ms^{-1}, the pyramidal cells fire perfectly synchronous bursts across all burst modes as g_{inh} is varied from 0.7 mS cm^{-2} for single spikes (figure 3(*b*), first panel) to 0 mS cm^{-2} for complex bursts (second panel). We note that for all lower values of β_{inh_c} perfectly synchronous bursting is also stable. Furthermore, as the decay rate β_{inh_c} gets smaller, perfect synchronization of initially unsynchronized cells occurs over fewer burst cycles. Presumably, similar synchronization results may be obtained with fast-decaying inhibition if additional currents, such as a sag current, are included in the cell models (Rubin and Terman 2000).

In this network, in contrast to the previous networks considered, burst frequency is determined by synaptic properties rather than pyramidal cell properties. Specifically, the decay rate of the common inhibition determines bursting frequency. For this reason, the frequency of each burst mode is much lower in this network compared to the corresponding frequencies in the previous networks. For example, with $\beta_{inh_c} = 0.005$ ms^{-1}, the frequencies range from 1.34 Hz for complex bursting ($g_{inh} = 0$ mS cm^{-2}) to 1.78 Hz for single spiking ($g_{inh} = 0.7$ mS cm^{-2}).

Previous synchronization studies have described how successful maintenance of synchrony by inhibition depends on the timescale of decay of the inhibition (van Vreeswijk *et al* 1994, Terman *et al* 1998). In particular, the inhibition must slowly decay over the entire duration of the silent phase. If the inhibition decays too quickly, there may not be sufficient compression of the time separation between cells, which may lead to a near-synchronous solution. Since the interburst interval in the single-spiking mode is significantly shorter than in the complex bursting mode, the common inhibition can compress spike firing times more closely together than complex burst firing times. For example, if $\beta_{inh_c} = 0.05$ ms^{-1} (figure 3(*c*)), inhibition decays too quickly to fully synchronize either the bursting or spiking solutions. The separation between firing times of the pyramidal cells changes, however, with the strength of local inhibition g_{inh}. Specifically, in the single-spiking mode ($g_{inh} = 0.7$ mS cm^{-2}, figure 3(*c*), first panel) spikes are fired within 1 ms of each other while there is approximately 10 ms separating firing times in the complex bursting mode ($g_{inh} = 0$ mS cm^{-2}, second panel). A difference between this near-synchronous bursting solution of network 3 and the near-synchronous bursting in network 1 is that the burst profiles in the pyramidal cells are identical in network 3 (compare figure 3(*c*), second panel and figure 1(*g*), first panel).

If initially the firing times of the pyramidal cells are close, the network will be attracted to either the perfectly synchronized bursting mode or the near-synchronous bursting mode, depending on the decay rate of the common inhibition. But, if the firing times of the pyramidal cells are initially far apart, the network may be attracted to a stable, anti-phase bursting mode. The existence of a stable anti-phase solution is similar to results obtained for networks of

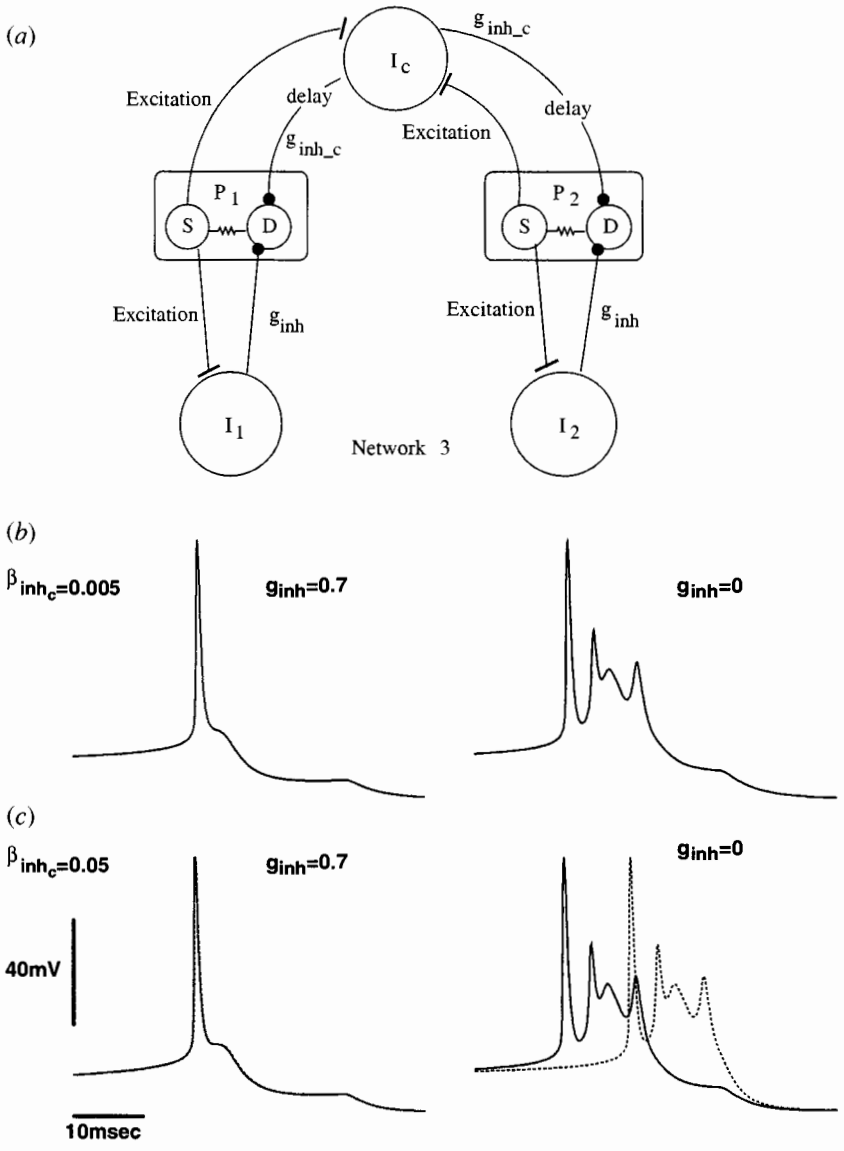

Figure 3. (*a*) A schematic diagram of model network 3. (*b*), (*c*) Pyramidal cell somatic voltage traces of perfectly synchronous bursting (*b*), obtained with a slow decay rate of common inhibition $\beta_{inh_c} = 0.005$ ms^{-1}, and near-synchronous bursting (*c*), obtained for a larger decay rate $\beta_{inh_c} = 0.05$ ms^{-1}, in the single-spiking mode ($g_{inh} = 0.7$ mS cm^{-2}, first panels) and in the complex bursting mode ($g_{inh} = 0$ mS cm^{-2}, second panels) (solid traces: leader cell; dotted traces: follower cell). The synaptic delay from the common interneuron I_c to the pyramidal cells is 20 ms. Arrival of the common inhibitory input to the cells is indicated by the dip in voltage following the spikes or bursts.

one-compartment neuron models (Terman *et al* 1998), so the bistability of solutions is not altogether unexpected. Simulation results indicate that the anti-phase solutions in network 3 have larger basins of attraction for burst modes with larger interburst intervals but the basins shrink as the decay rate of common inhibition decreases.

3.3. Synchronizing influence of common inhibition can drive perfect synchrony in the presence of recurrent synaptic excitation

In the above sections, we considered networks where either recurrent excitation or common inhibition was the mechanism synchronizing firing. We now consider a network in which both mechanisms are present, specifically two pyramidal cell–interneuron subcircuits reciprocally coupled to a common interneuron and also with recurrent excitatory synapses targeting the dendrite compartments (network 4, figure 4(*a*)). This network is identical to network 3 except with recurrent excitatory connections added between the pyramidal cells. As described above, recurrent excitation acting during the active phase of bursting tends to desynchronize pyramidal cell firing and promotes near-synchronous bursting. Common, slowly decaying inhibition that is delayed so that it acts during the silent phase of bursting can bring firing times closer together and promotes perfectly synchronous bursting. When the decay rate of the common inhibition is very slow in network 4, then the desynchronization that occurs during the active phase can be overcome during the silent phase and perfectly synchronous bursting is stable for any level of net local inhibition. In particular, with the decay rate β_{inh_c} set to 0.0001 ms^{-1}, the network displays perfectly synchronized bursting (figure 4(*b*)) in all modes from complex bursting (second panel) to single spiking (first panel) as the strength of the recurrent excitation, g_{exc}, varies between 4.5 and 0 mS cm^{-2} for a fixed strength of local inhibition ($g_{inh} = 0.7$ mS cm^{-2}). The bursting frequencies, since they are primarily governed by β_{inh_c}, are extremely low at approximately 0.045 Hz for all bursting modes.

For the decay rate $\beta_{inh_c} = 0.0005$ ms^{-1}, if recurrent excitation were not present between pyramidal cells, common inhibition could perfectly synchronize firing. If, however, there is even very weak recurrent excitation between the cells, the network displays near-synchronous bursting (figure 4(*c*)). For $g_{exc} = 0.3$ mS cm^{-2}, at which the pyramidal cells fire single spikes (with fixed strength of local inhibition $g_{inh} = 0.7$ mS cm^{-2}), the desynchronizing effect of the recurrent excitation is weak and the common inhibition can bring firing times within 1 ms of each other (figure 4(*c*), first panel). For strong recurrent excitation ($g_{exc} = 3.5$ mS cm^{-2}, second panel), the separation of the burst trajectories during the active phase cannot be reduced during the silent phase; thus complex burst firing times remain approximately 2 ms apart and burst profiles retain their differences. We note that the complex burst profiles in this case are similar to those displayed by network 1 (compare figure 4(*c*), second panel, to figure 1(*h*), third panel) since the common inhibition acts during the silent phase of bursting and does not have a significant effect on the active phase. We further remark that since the timings of the recurrent excitation and local inhibition in the perfectly synchronous firing mode and in the follower cell in the near-synchronous bursting mode are similar, these complex burst profiles are more similar to one another than to the profile of the leader cell in the near-synchronous bursting mode (compare figure 4(*b*), second panel, to figure 4(*c*), second panel).

A result of including recurrent excitation in network 4 is that the anti-phase bursting state that was a second stable solution in network 3 may no longer exist. Very weak recurrent excitation, for example $g_{exc} = 0.2$ mS cm^{-2}, can pull firing times together and drive more synchronous firing.

3.4. Equivalent networks with different architectures display the same firing patterns

In networks 1 and 2, each pyramidal cell is paired with an interneuron that provides fast, local inhibition that contributes to the modulation of the burst firing pattern. Obtaining similar synchronous firing patterns in a larger network consisting of many more pyramidal cells would presumably require individual local interneurons for each pyramidal cell. However,

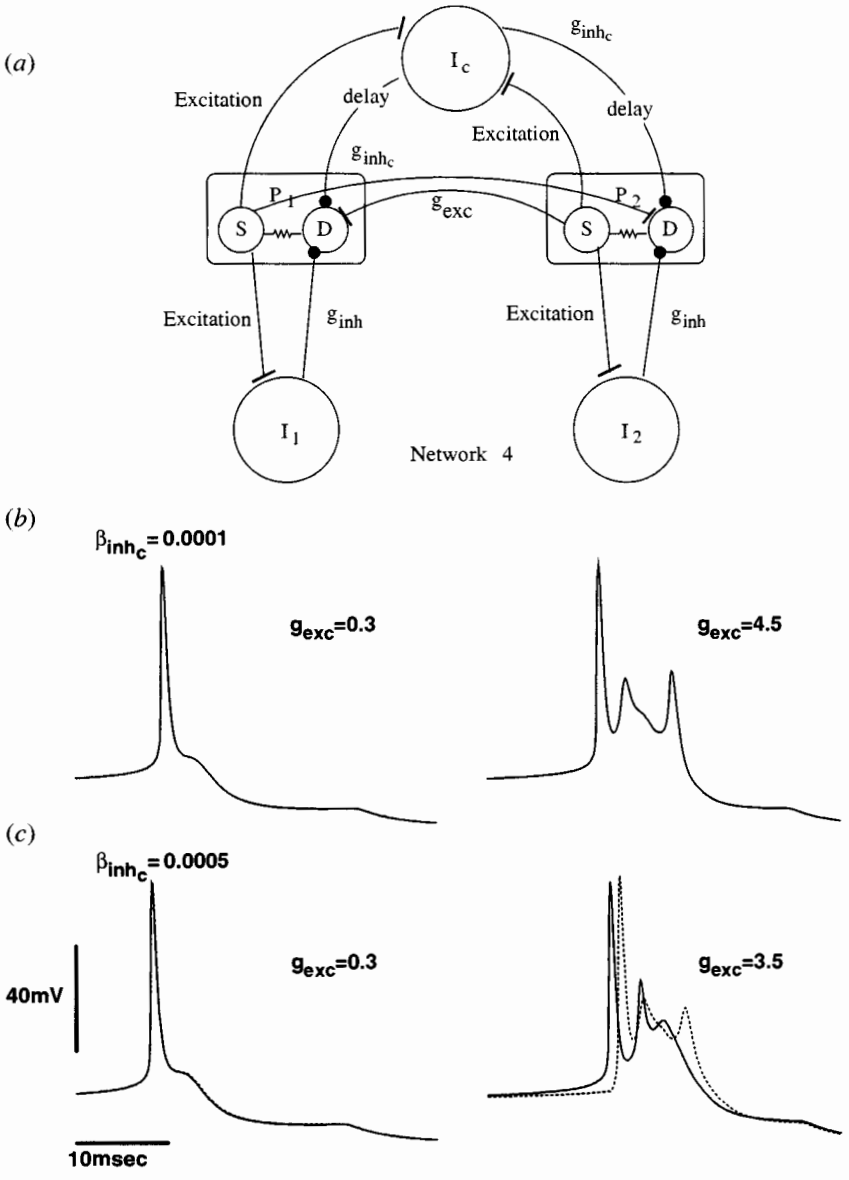

Figure 4. (*a*) A schematic diagram of model network 4. (*b*), (*c*) Pyramidal cell somatic voltage traces of perfectly synchronous bursting (*b*), obtained with a slow decay rate of common inhibition $\beta_{inh_c} = 0.0001$ ms^{-1}, and near-synchronous bursting (*c*), obtained for a larger decay rate $\beta_{inh_c} = 0.0005$ ms^{-1}, in the single-spiking mode ($g_{exc} = 0.3$ mS cm^{-2}, first panels) and in the complex bursting mode ($g_{exc} = 4.5$ (*b*) and $g_{exc} = 3.5$ (*c*) mS cm^{-2}, second panels, $g_{inh} = 0.7$ mS cm^{-2}) (solid traces: leader cell; dotted traces: follower cell). The synaptic delay from the common interneuron I_c to the pyramidal cells is 20 ms.

in region CA3, pyramidal cells outnumber interneurons with a ratio of approximately 9–1. Thus, it is most probably unrealistic to assume that burst firing is modulated via a one-to-one pairing of interneurons with pyramidal cells. Our above analyses of networks 1 and 2 indicate that the synchrony pattern obtained essentially depends on the relative timing of

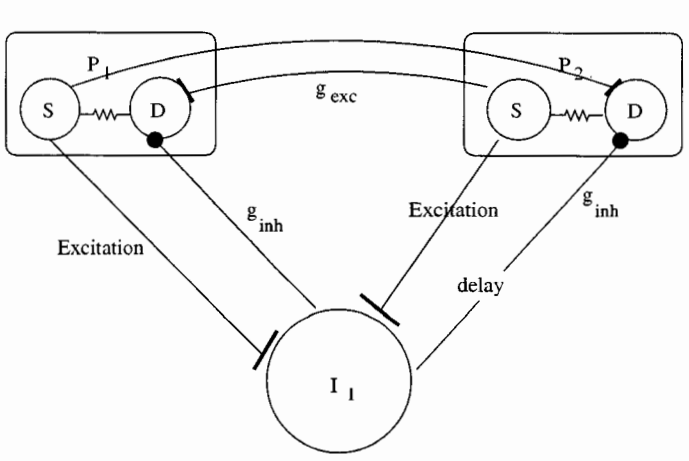

Figure 5. A schematic diagram of a network with a firing dynamics equivalent to that of network 1.

arrival of synaptic excitation and inhibition, and whether that timing allows for activation of the dendritic calcium-based spike. Applying these insights, we propose that different network architectures that do not have one-to-one pairing of pyramidal cells and interneurons but that may incorporate synaptic delays can exhibit bursting patterns identical to those displayed by networks 1 and 2.

One such network consists of two pyramidal cells with recurrent excitatory synaptic connections targeting their dendrite compartments and with reciprocal synaptic connections onto a single interneuron. When a synaptic delay in the connection from the interneuron to the dendrite compartment of one of the pyramidal cells is present, perhaps due to an indirect synapse, this network (figure 5) displays near-synchronous bursting as in network 1. The length of the delay can vary between 1 and 5 ms. In this network, the interneuron provides the same inhibition at the same time to the leader cell as the leader interneuron does in network 1. While the local inhibitory current targeted on the follower cell is activated by the leader burst, due to the synaptic delay, it arrives at the follower cell at approximately the same time as in network 1. In fact, with a synaptic delay of 2 ms, the voltage traces for this network are nearly identical to the traces for network 1 across several burst modes as g_{exc} is varied. For this reason, we claim that this network is 'equivalent' to network 1 in that the same firing dynamics are achieved by networks with different architectures.

There is, however, a difference in architectural symmetry of these two networks that has implications for the firing patterns. The symmetric synaptic connections in network 1 allow for either pyramidal cell to lead the burst firing. The initial conditions from which the firing is initiated determine the firing order. The synaptic delay in the equivalent network introduces an asymmetry in the network dynamics that forces the pyramidal cell receiving the delayed inhibition to be the follower cell.

We also note that the networks have equivalent dynamics when they are firing in the near-synchronous bursting mode. If other synaptic inputs were introduced or if other elements were changed in the networks that destabilize near-synchronous bursting, we would not necessarily expect the two networks to change their firing patterns in the same way. For example, if the recurrent excitation between pyramidal cells is blocked in network 1, the two pyramidal cells uncouple and fire independently. If the same change is to made to the

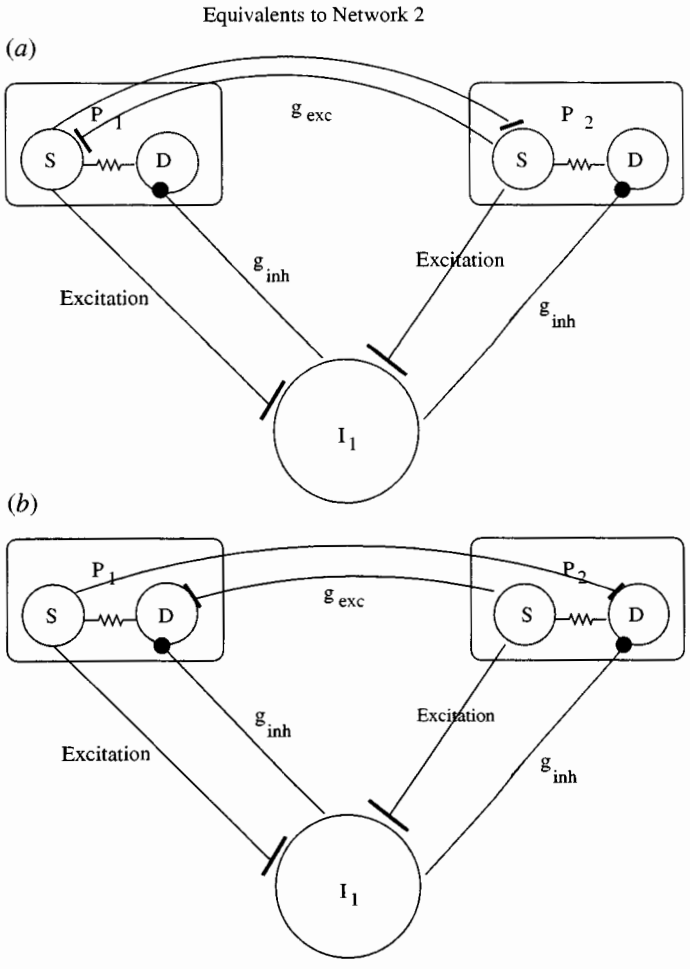

Figure 6. (*a*), (*b*) Schematic diagrams of two networks with equivalent firing dynamics to network 2.

equivalent network, the pyramidal cells remain coupled through the common interneuron. Depending on the length of the delay and the strength of the inhibition, firing of the follower cell can be suppressed.

A network equivalent to network 2 consists of two pyramidal cells with recurrent excitatory synapses targeting the soma compartments and with reciprocal connections to a single interneuron (figure 6(*a*)). This network displays burst-envelope synchrony with voltage traces nearly identical to those of network 2 across all burst modes as g_{exc} is varied. No synaptic delays are included in this network, so the two pyramidal cells receive local inhibition at the same time. In the follower cell, this inhibition arrives slightly earlier than it does in network 2, but still allows for the activation of a single somatic spike.

Another equivalent network that displays very similar burst-envelope synchronous firing to network 2 across all burst modes is the same as the above equivalent network except that the recurrent excitation targets the dendrite compartments (figure 6(*b*)). This network architecture resembles that of the equivalent network for network 1 above, but there are no delays from the interneuron to either pyramidal cell. Although, in this network, the recurrent excitation

arriving at the dendrite compartments promotes full expression of the dendritic spike, in the follower cell the local inhibition arrives sufficiently early with respect to the recurrent excitation to suppress it.

4. Discussion

By investigating different pyramidal cell–interneuron networks, we have shown that recurrent excitation between pyramidal cells, while able to pull firing times close, generally does not lead to perfectly synchronous firing times. The synaptic excitation arriving during burst firing of the pyramidal cells causes differences in burst profiles and subsequent interburst intervals that drive firing times apart. Additional inhibitory synaptic inputs that arrive during the burst via subcircuits with local interneurons may further modulate burst profiles and interburst intervals depending on their timing relative to the excitatory synaptic inputs. Specifically, if these inputs suppress dendritic depolarization in one of the pyramidal cells, burst profiles can be significantly different.

We have shown that common inhibition can perfectly synchronize bursting of pyramidal cells, but burst frequencies are low. With faster decay rates of common inhibition and, thus, faster frequencies, it can bring firing times close together and, interestingly, the time separation depends on the burst firing mode. When both recurrent excitation and common inhibition are present, very slow decay rates of the common inhibition are necessary for perfect synchrony. But with larger values of the decay rate, common inhibition can pull firing times closer together than recurrent excitation alone, especially in the single-spike bursting mode (compare figure 4(*c*), first panel, with figure 1(*f*)).

Many previous synchronization studies have focused either on the role of excitation or that of inhibition, and often on their roles synchronizing a specific type of neuronal firing pattern such as bursting or spiking. These studies have used either spiking neuron models (van Vreeswijk *et al* 1994, Hansel *et al* 1995, Gerstner *et al* 1996, Chow 1998) or conductance-based, yet idealized relaxation oscillator models (Somers and Kopell 1993, Terman *et al* 1998, Bose *et al* 2000, Rubin and Terman 2000). Due to the particular focus of these works, it is often straightforward to understand and interpret their findings. For example, for certain relaxation oscillator models Somers and Kopell (1993) show that excitation can perfectly synchronize burst envelopes. The works on spiking neurons, however, suggest that excitation desynchronizes neurons (van Vreeswijk *et al* 1994, Hansel *et al* 1995, Ermentrout 1996). These results are not inconsistent since the type of firing considered is different for each case. In this paper, our use of the two-compartment Pinsky–Rinzel pyramidal cell model allows us to explore synchronization questions across different burst and spiking modes using a single model cell. For example, we show that recurrent excitation cannot perfectly synchronize bursting cells, but can synchronize spiking cells, provided the excitation targets the soma compartment of the cell (compare figures 1(*f*) and 2(*f*)), and that the dendrite also spikes. This can occur whether spiking is induced by high somatic applied current or is a result of strong local inhibition. Other studies of synchrony of single spikes by excitation have suggested that perfect synchrony is not stable unless the synapses are extremely fast (van Vreeswijk *et al* 1994, Hansel *et al* 1995). This contrasts with our finding (figure 2(*f*)), as the synaptic rise and decay rates (2 and 1 ms^{-1}, respectively) are not unusually fast. Our work also shows that the presence of excitation alone does not necessarily desynchronize cells, as slowly decaying inhibition may be strong enough to counteract its effect. Thus, we suggest that certain general rules obtained from prior modelling studies may not necessarily hold in more realistic neuronal models that have both excitatory and inhibitory network components.

A primary focus of this work has been to show that the timing of synaptic events relative to one another and to intrinsic cell events can strongly determine the type of network behaviour observed. Indeed, the timing of input which instigates, modulates or suppresses the dendritic calcium event has profound influence on synchronous firing. Small changes in the timing of inputs that affect calcium-based burst dynamics (e.g. removal of synaptic delays in figures 5 and 6(*b*)) can move the network from nearly synchronous to burst-envelope synchronous firing. That the network output can be so easily manipulated makes networks consisting of such neurons good candidates for conveying both firing rate and temporal codes. In the former case, the type of synchrony (near versus perfect, for example) may not be so relevant as simply the number of spikes emitted within a given time window. In the latter case, the interspike interval may encode information about the activity of upstream neurons. In this way, a single firing pattern can convey two different pieces of information to two different downstream sites in a way that each of the pieces of information can be modulated without affecting the other. For example, a detector that measures the interspike interval of the first spike of a burst would not discriminate between near synchronous or burst-envelope synchronous firing, but a firing rate detector would. Similarly, a firing rate detector would be little affected by differences between near and perfectly synchronous solutions, but an interspike interval detector would be affected.

Emphasis on timing has also allowed us to identify groups of equivalent networks, where architecture may not be uniquely determined from observation of a single firing pattern. Equivalent networks have the advantage that they can display identical stable firing patterns, but each may be capable of producing completely different and independent outputs. This could depend on the nature of the bistability that may exist within each of the networks, or on the outside inputs which may drive the network. For example, it is well established that the firing of CA3 pyramidal cells codes for spatial location in freely moving rats (O'Keefe and Dostrovsky 1971). A specific set of cells can be part of a larger cell assembly that codes for a specific location. This set would then be considered an equivalent subnetwork of the cell assembly. However, cells can and do fire in more than one spatial location. The set of cells in question may also fire together with another cell assembly and thus be an equivalent subnetwork of that assembly. The firing patterns of these cell assemblies need not be identical. The difference in firing patterns of the specific set of cells in question could be a function of which other cells are driving them and the nature of the timing of intrinsic and synaptic events within a given cell assembly. In this way a subset of cells could participate in two different coding activities by being equivalent to two different networks, neither of which is necessarily equivalent to the other.

The ideas presented in this paper may be useful in understanding how certain dynamic firing patterns are generated in various regions of the brain. In the neocortex, for example, many different types of synapse have been reported to have depressing or facilitating dynamics (Thomson and Deuchars 1994, Markram *et al* 1998). In particular, synapses between pyramidal cells show frequency-dependent depression (Thomson 1997). In the hippocampus, the activity dependence of synaptic transmission has not been as heavily investigated; however, synaptic depression within interneuron networks in the dentate gyrus (Bartos *et al* 2001) and frequency-dependent modulation of post-synaptic potentials in CA1 pyramidal neurons (Bracci *et al* 2001) have recently been reported. As is evident in figures 1(*b*)–(*f*) and 2(*b*)–(*f*), a change in the net synaptic input arriving during burst firing can lead to a change in burst firing rate. For example, if, during repetitive bursting of a network of pyramidal cells, the net synaptic inhibition arriving during burst firing increased, the rate of burst firing in the network would also increase. In the networks considered here, especially networks 1 and 2, if either the recurrent excitatory synapses or the local inhibitory synapses

showed activity-dependent depression, the network would display a self-generated change in firing rate.

By focusing attention on two-compartment models, we have shown how and why various patterns of firing and synchrony can arise. Our results emphasize the importance of timing and location of synaptic events for firing patterns. The present work suggests that the details of the firing patterns together with the type of synchrony can have functional implications as regards the amount of information that a network is able to convey.

Acknowledgment

This research was supported by a grant from the National Science Foundation (DMS-9973230 (VB, AB)).

References

Bartos M, Vida I, Frotscher M, Geiger J R P and Jonas P 2001 Rapid signaling at inhibitory synapses in a dentate gyrus interneuron network *J. Neurosci.* **21** 2687–98

Booth V and Bose A 2001a Neural mechanisms for generating rate and temporal codes in model CA3 pyramidal cells *J. Neurophysiol.* **85** 2432–45

Booth V and Bose A 2001b Regulating firing rate of networks of pyramidal cells *Neurocomputing* **38–40** 497–504

Bose A and Booth V 2002 Analysis of excitation induced desynchronization of two-compartment pyramidal cells, in preparation

Bose A, Kopell N and Terman D 2000 Almost-synchronous solutions for mutually coupled excitatory neurons *Physica* D **140** 69–94

Bracci E, Vreugdenhil M, Hack S P and Jefferys J G R 2001 Dynamic modulation of excitation and inhibition during stimulation at gamma and beta frequencies in the CA1 hippocampal region *J. Neurophys.* **85** 2412–22

Butera R J, Rinzel J and Smith J C 1999 Models of respiratory rhythm generation in the pre-Botzinger complex: II. Populations of coupled pacemaker neurons *J. Neurophys.* **82** 398–415

Chow C 1998 Phase locking in weakly heterogeneous neuronal networks *Physica* D **118** 343–70

Ermentrout G B 1996 Type I membranes, phase resetting curves and synchrony *Neural Comput.* **8** 979–1001

Ermentrout G B and Kopell N 1998 Fine structure of neural spiking and synchronization in the presence of conduction delays *Proc. Natl Acad. Sci. USA* **95** 1259–64

Gerstner W, van Hemmen J L and Cowan J D 1996 What matters in neuronal locking? *Neural Comput.* **8** 1653–76

Hansel D, Mato G and Meunier C 1995 Synchrony in excitatory neural networks *Neural Comput.* **7** 307–35

Markram H, Wang Y and Tsodyks M 1998 Differential signaling via the same axon of neocortical pyramidal neurons *Proc. Natl Acad. Sci. USA* **95** 5323–28

Menschik E D, Yen S C and Finkel L H 1999 Model- and scale-independent performance of a hippocampal CA3 network architecture *Neurocomputing* **26–7** 443–53

Morris C and Lecar H 1981 Voltage oscillations in the barnacle giant muscle fiber *Biophys. J.* **35** 193–213

O'Keefe J and Dostrovsky J 1971 The hippocampus as a spatial map. Preliminary evidence from unit activity in the freely-moving rat *Brain Res.* **34** 171–5

Pinsky P F and Rinzel J 1994 Intrinsic and network rhythmogenesis in a reduced Traub model for CA3 neurons *J. Comput. Neurosci.* **1** 39–60

Pinsky P F and Rinzel J 1995 *J. Comput. Neurosci.* **2** 275 (erratum)

Rubin J and Terman D 2000 Geometric analysis of population rhythms in synaptically coupled neuronal networks *Neural Comput.* **12** 597–645

Somers D and Kopell N 1993 Rapid synchronization through fast threshold modulation *Biol. Cybern.* **68** 393–407

Terman D, Kopell N and Bose A 1998 Dynamics of two mutually coupled slow inhibitory neurons *Physica* D **117** 241–75

Thomson A M 1997 Activity-dependent properties of synaptic transmission at two classes of connections made by rat neocortical pyramidal axons *in vitro J. Physiol.* **502.1** 131–47

Thomson A M and Deuchars J 1994 Temporal and spatial properties of local circuits in neocortex *Trends. Neurosci.* **17** 119–26

Tiesinga P H E, Fellous J-M, Jose J V and Sejnowski T J 2001 Computational model of carbachol-induced delta, theta and gamma oscillations in the hippocampus *Hippocampus* **11** 251–74

Traub R D and Bibbig A 2000 A model of high-frequency ripples in the hippocampus based on synaptic coupling plus axon–axon gap junctions between pyramidal cells *J. Neurosci.* **20** 2086–93

Traub R D, Wong R, Miles R and Michelson H 1991 A model of a CA3 hippocampal pyramidal neuron incorporating voltage-clamp data on intrinsic conductances *J. Neurophysiol.* **66** 635–49

van Vreeswijk C, Abbott L and Ermentrout G B 1994 When inhibition, not excitation synchronizes neural firing *J. Comput. Neurosci.* **1** 313–21

Wennekers T and Sommer F T 1999 Gamma-oscillations support optimal retrieval in associative memories of two-compartment neurons *Neurocomputing* **26–7** 573–8

Ylinen A, Bragin A, Nadasy Z, Jando G, Szabo I, Sik A and Buzsaki G 1995 Sharp wave-associated high-frequency oscillation (200 Hz in the intact hippocampus: network and intracellular mechanism *J. Neurosci.* **15** 30–46